Nano Research
2020, 13(12): 3235–3240
ISSN 1998-0124 CN 11-5974/O4
https://doi.org/10.1007/s12274-020-2995-2

Research Article

Giant pattern evolution in third-harmonic generation of strained monolayer WS_2 at two-photon excitonic resonance

Jing Liang[1,2,§], He Ma[1,2,§], Jinhuan Wang[3], Xu Zhou[1], Wentao Yu[1], Chaojie Ma[1], Muhong Wu[1], Peng Gao[4], Kaihui Liu[1,2] (✉), and Dapeng Yu[5]

[1] *State Key Laboratory for Mesoscopic Physics and Frontiers Science Center for Nano-optoelectronics, School of Physics, Peking University, Beijing 100871, China*
[2] *Academy for Advanced Interdisciplinary Studies, Collaborative Innovation Center of Quantum Matter, Peking University, Beijing 100871, China*
[3] *School of Chemistry and Chemical Engineering, Beijing Institute of Technology, Beijing 100081, China*
[4] *International Center for Quantum Materials, Electron Microscopy Laboratory, School of Physics, Peking University, Beijing 100871, China*
[5] *Shenzhen Institute for Quantum Science and Engineering, and Department of Physics, Southern University of Science and Technology, Shenzhen 518055, China*
[§] *Jing Liang and He Ma contributed equally to this work.*

Received: 5 May 2020 / **Revised:** 6 July 2020 / **Accepted:** 19 July 2020

ABSTRACT

Strong geometrical confinement and reduced dielectric screening of two-dimensional (2D) materials leads to strong Coulomb interaction and eventually give rise to extraordinary excitonic effects, which dominates the optical and optoelectronic properties. For nonlinear 2D photonic or optoelectronic applications, excitonic effects have been proved effective to tune the light-matter interaction strength. However, the modulation of excitonic effects on the other aspect of nonlinear response, i.e., polarization dependence, has not been fully explored yet. Here we report the first systemic study on the modulation of excitonic effects on the polarization dependence of second and third harmonic generation (SHG and THG) in strained monolayer WS_2 by varying excitation wavelength. We demonstrated that polarization-dependent THG patterns undergo a giant evolution near two-photon excitonic resonance, where the long-axis of the parallel component (originally parallel to the strain direction) has a 90° flip when the excitation wavelength increases. In striking contrast, no apparent variation of polarization-dependent SHG patterns occurs at either two- or three-photon excitonic resonance conditions. Our results open a new avenue to modulate the anisotropic nonlinear optical response of 2D materials through effective control of excitonic resonance states, and thus open opportunity for new designs and applications in nonlinear optoelectronic 2D devices.

KEYWORDS

two-dimensional materials, nonlinear optics, excitonic effects

1 Introduction

Nonlinear optics is an essential part of modern optics and plays a crucial role in various optical applications including ultrafast pulse laser generation, optical parametric generation/amplification, optical switches, optical modulators and so forth [1–3]. Nowadays, the increasing development trend of miniaturization and on-chip integration of photonic devices implies high demand on new nonlinear medium with strong nonlinearity even at small size [4–6]. The rising two-dimensional (2D) materials provide a novel platform to study numerous nonlinear optical effects due to large nonlinear susceptibility, ultrafast recovery time and large optical/thermal damage threshold [7–12]. From desirable application point of view, it is a prerequisite to effectively tune and modulate the nonlinear optical response of 2D materials.

There are two dimensions of modulation on the nonlinear optical response of 2D materials: nonlinearity enhancement and polarization dependence. The former issue devotes to breaking the limitation of weak conversion efficiency due to atomically thin light-matter interaction length. In addition to conventional waveguide integration, plasmonic enhancement and optical resonator, the strong Coulomb interaction due to strong geometrical confinement and reduced dielectric screening in low dimensions adds a new freedom: strong excitonic effects [13–20]. The underlying mechanism is that the magnitude of nonlinear susceptibility could be dramatically enhanced when the exciton state is coincident with intermediate states in the nonlinear optical process. As for the modulation of polarization dependence for anisotropic nonlinear optical applications, the cornerstone is that polarization dependence usually relies on crystallographic symmetry of 2D materials [21, 22]. Therefore, symmetry-related methods are wildly utilized, such as crystallographic orientation, interlayer stacking order, phase transition and strain tensor [23–27]. However, the majority of works to date mainly specializes only one aspect of modulation. It is well known that excitonic effects dominate the optical and optoelectronic properties of 2D semiconducting

Address correspondence to khliu@pku.edu.cn

materials. Therefore, the impact of unique excitonic effects in 2D materials on the other aspect, i.e., polarization dependence of nonlinear response, should not be ignored and need to be fully explored.

In order to experimentally reveal the regulation of excitonic effects on the polarization dependence of nonlinear optical response, the 2D material should satisfy the following requirements: (i) strong excitonic effects; (ii) a proper optical bandgap for easily achieving excitonic resonance; (iii) more than one independent non-zero element in the nonlinear susceptibility tensor to guarantee that each element could freely vary with excitation wavelength. Therefore, strained monolayer tungsten disulfide (WS_2) should be the optimal candidate due to suitable direct optical bandgap and large second/third order nonlinear susceptibilities [28–31]. In addition, the uniaxial tensile strain reduces the crystallographic symmetry and eventually breaks the constraint between susceptibility tensor elements [25, 26].

In this work, we report a systemic study of excitonic effect on the polarization-dependent second/third harmonic generation (SHG/THG) patterns of strained monolayer WS_2 through different excitation wavelength. We find that THG goes through a dramatic pattern evolution around two-photon excitonic resonance. In particular, the long-axis of the parallel component, which has an obvious correspondence with strain direction, has a 90° flip; the long-axis and short-axis of the perpendicular component interchange with each other. Nevertheless, SHG patterns seem more robust and do not show apparent variation with excitation wavelength. Therefore, our results demonstrate that excitonic effects have a significant modulation on polarization dependence of THG response. From a characterization point of view, the excitonic effects should be carefully taken into consideration when employing nonlinear optics to unveil symmetry-related properties. Moreover, our results also provide a novel perspective to tune anisotropic nonlinear optical response of 2D materials through effectively modulating the excitonic resonance state, which would facilitate new applications based on 2D materials in the future nonlinear optoelectronic devices.

2 Experimental

2.1 CVD growth of monolayer WS_2 flakes

Chemical vapour deposition (CVD) method was used to grow monolayer WS_2 flakes on SiO_2/Si substrate. The precursors WO_3 powder (10.0 mg) and NaCl powder (1.5 mg) were placed in quartz boat at center of the tube furnace. S powder (30.0 mg) was placed at the upstream while the substrate was placed upon the quartz boat at the downstream of the CVD system. The procedure is as follows: keep at 105 °C with 500 sccm Ar flow for 1 h, ramp to 800 °C with 15 sccm Ar flow in 50 min, keep at 800 °C with 250 sccm Ar flow for 10 min, and then naturally cool down to room temperature. To apply uniaxial tensile strain onto monolayer WS_2 flakes, the samples were transferred onto the flexible Acrylic substrate using a polymethyl methacrylate (PMMA)-assisted transfer method.

2.2 Nonlinear optical characterization.

Femtosecond pulse laser at 800 nm (~ 100 fs, 76 MHz) is generated by a Ti: sapphire oscillator (Coherent Mira-HP). Equipped with an optical parametric oscillator (Coherent Mira-OPO-X), signal beam (1,000–1,600 nm) and idler beam (1,750–4,000 nm) could be used to excite monolayer WS_2. With normally incident configuration, the linear polarization of excitation beam is controlled by a half-wave plate in front of the objective (40×, N.A.= 0.65). In reflection geometry, a linear analyzer parallel (perpendicular) to the incident polarization is utilized to extract the parallel (perpendicular) component $I^{\parallel}$ ($I^{\perp}$) of SHG/THG generated from the sample. In the end, SHG/THG pattern is obtained by a grating spectrograph with CCD (Princeton SP-2500i) to record the SHG/THG intensity as a function of polarization angle.

3 Results and discussions

3.1 Basic optical properties of monolayer WS_2

Spectroscopy approaches provide a versatile tool for in-depth characterization of our high-quality CVD grown monolayer WS_2 (Fig. 1(a)). In Raman spectrum, the characteristic in-plane vibration E^1_{2g} mode ~ 356 cm^{-1} and out-of-plane A_{1g} mode ~ 417 cm^{-1} provide a structural fingerprint to identify the monolayer WS_2 (Fig. 1(b)). The pronounced peak ~ 622 nm in photoluminescence (PL) spectrum corresponds to A-exciton and indicates the direct optical bandgap of monolayer WS_2 (Fig. 1(c)). SHG/THG is a nonlinear optical process in which two/three incident photons (ω, λ) are converted to a single new photon (2ω, $\lambda/2$)/(3ω, $\lambda/3$) through nonlinear interaction with a material. In our experiment, under excitation of a normally-incident linearly-polarized pulse laser (λ_{ex} = 1,200 nm/ 1,240 nm), both SHG (600 nm/620 nm) and THG (400 nm/ 413 nm) signal from monolayer WS_2 could be collected in reflection geometry (Fig. 1(d)). Obviously, the SHG/THG intensity is significantly enhanced around the two-photon excitonic resonance (λ_{ex} = 1,240 nm) due to two-photon excitonic resonance. That is, SHG/THG conversion efficiency or the effective nonlinearity of monolayer WS_2 could be strongly modulated by excitonic resonance. In the following, to reveal the impact of excitonic on the polarization dependence of nonlinear optical response, SHG/THG patterns under different excitation wavelength are systemically studied.

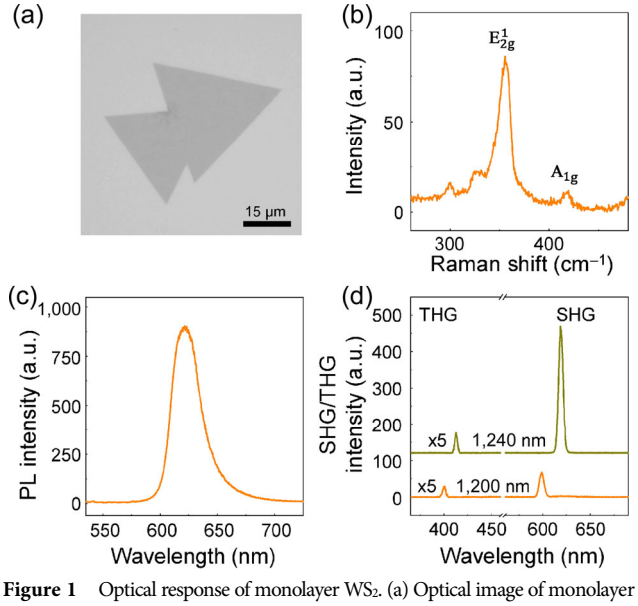

Figure 1 Optical response of monolayer WS_2. (a) Optical image of monolayer WS_2. The scale bar is 15 μm . (b) Raman spectrum of monolayer WS_2 with two characteristic peaks E^1_{2g} mode ~ 356 cm^{-1} and A_{1g} mode ~ 417 cm^{-1}. (c) PL spectrum of monolayer WS_2. The PL peak at ~ 622 nm indicates the direct optical bandgap. (d) Nonlinear optical response SHG/THG of monolayer WS_2 at different excitation laser wavelength. The sharp peak centered at 600 nm/400 nm or 620 nm/413 nm is SHG/THG signal under 1,200 or 1,240 nm excitation. The THG signal is scaled up by a factor of 5.

3.2 Symmetry description of polarization-dependent SHG/THG patterns of intrinsic and strained monolayer WS_2

In our experiment, when a fundamental laser beam ω has a nonlinear interaction with monolayer WS_2, the generated SHG/THG intensity could be expressed as

$$I(n\omega) = \left| \hat{\boldsymbol{e}}_{n\omega} \chi^{(n)} \hat{e}_{\omega}^{n} \right|^2 \tag{1}$$

where $\chi^{(n)}$ is the second/third ($n = 2/n = 3$) order nonlinear optical susceptibility of monolayer WS_2, $\hat{\boldsymbol{e}}_{\omega} = (-\sin\varphi \quad \cos\varphi)$ is the unit polarization vector of incident light, φ is the incident light polarization angle relative to armchair direction, $\hat{\boldsymbol{e}}_{n\omega}$ is the unit polarization vector of the generated SHG/THG ($n = 2/n = 3$) signal. When $\hat{\boldsymbol{e}}_{n\omega} = (-\sin\varphi \quad \cos\varphi)$ or $\hat{\boldsymbol{e}}_{n\omega} = (\cos\varphi \quad \sin\varphi)$, the parallel or perpendicular component of the polarization-dependent SHG/THG patterns could be obtained. Due to the normal incidence along c-axis, all components in $\chi^{(n)}$ that contain an out-of-plane c term are set to zero since they do not contribute to the final SHG/THG response:

$$\chi^{(2)} = \begin{pmatrix} \chi_{aaa} & \chi_{aab} & \chi_{aba} & \chi_{abb} \\ \chi_{baa} & \chi_{bab} & \chi_{bba} & \chi_{bbb} \end{pmatrix},$$

$$\chi^{(3)} = \begin{pmatrix} \chi_{aaaa} & \chi_{aaab} & \chi_{aaba} & \chi_{abaa} & \chi_{aabb} & \chi_{abab} & \chi_{abba} & \chi_{abbb} \\ \chi_{baaa} & \chi_{baab} & \chi_{baba} & \chi_{bbaa} & \chi_{babb} & \chi_{bbab} & \chi_{bbba} & \chi_{bbbb} \end{pmatrix} \tag{2}$$

where a and b represent the in-plane zigzag and armchair direction, respectively. Therefore, the polarization-dependent SHG/THG patterns has the following form:

$$\begin{aligned} I_{2\omega}^{\parallel} = & \left| -\chi_{aaa}\sin^3\varphi + (2\chi_{aab} + \chi_{baa})\sin^2\varphi\cos\varphi - \right. \\ & \left. (\chi_{abb} + 2\chi_{bab})\sin\varphi\cos^2\varphi + \chi_{bbb}\cos^3\varphi \right|^2 \\ I_{2\omega}^{\perp} = & \left| \chi_{baa}\sin^3\varphi + (\chi_{aaa} - 2\chi_{bab})\sin^2\varphi\cos\varphi + \right. \\ & \left. (\chi_{bbb} - 2\chi_{aab})\sin\varphi\cos^2\varphi + \chi_{abb}\cos^3\varphi \right|^2 \end{aligned}$$

$$\begin{aligned} I_{3\omega}^{\parallel} = & \left| \chi_{aaaa}\sin^4\varphi - (3\chi_{aaab} + \chi_{baaa})\sin^3\varphi\cos\varphi + \right. \\ & (3\chi_{aabb} + 3\chi_{baab})\sin^2\varphi\cos^2\varphi - \\ & \left. (\chi_{abbb} + 3\chi_{babb})\sin\varphi\cos^3\varphi + \chi_{bbbb}\cos^4\varphi \right|^2 \\ I_{3\omega}^{\perp} = & \left| -\chi_{baaa}\sin^4\varphi + (3\chi_{baab} - \chi_{aaaa})\sin^3\varphi\cos\varphi + \right. \\ & (3\chi_{aaab} - 3\chi_{babb})\sin^2\varphi\cos^2\varphi + \\ & \left. (\chi_{bbbb} - 3\chi_{aabb})\sin\varphi\cos^3\varphi + \chi_{abbb}\cos^4\varphi \right|^2 \end{aligned} \tag{3}$$

Intrinsic monolayer WS_2 belongs to non-centrosymmetric D_{3h} crystallographic point group. Hence the $\chi_{\text{int}}^{(n)}$ tensor could be further simplified according to crystallographic symmetry and permutation symmetry [21, 22]. $\chi_{\text{int}}^{(2)}$ and $\chi_{\text{int}}^{(3)}$ tensor elements are totally determined by one independent variable respectively: $\chi_{bbb} = -\chi_{baa} = -\chi_{aab} = -\chi_{aba} = A$; $\chi_{aaaa} = \chi_{bbbb} = \chi_{aabb} + \chi_{abab} + \chi_{abba} = \chi_{bbaa} + \chi_{baba} + \chi_{baab} = B$. Finally, polarization-dependent SHG/THG patterns of intrinsic monolayer WS_2 are given by

$$\begin{aligned} & I_{\text{int}}^{\parallel}(2\omega) = \left| A\cos 3\varphi \right|^2, \; I_{\text{int}}^{\perp}(2\omega) = \left| A\sin 3\varphi \right|^2; \\ & I_{\text{int}}^{\parallel}(3\omega) = B^2, \; I_{\text{int}}^{\perp}(3\omega) = 0. \end{aligned} \tag{4}$$

As expected, the parallel/perpendicular component of polarization-dependent SHG exhibits six-fold rotational symmetric pattern, and the maximum has a one-to-one correspondence with armchair/zigzag direction of monolayer WS_2 (Figs. 2(a)–2(c)). The generated THG signal has the same polarization as incident light so that polarization-dependent THG only has the parallel component, which exhibits a perfect circle (Figs. 2(d) and 2(e)). Obviously, since non-zero elements in $\chi_{\text{int}}^{(2)}$ or $\chi_{\text{int}}^{(3)}$ tensor are constrained by the only one independent variable A or B, SHG/THG patterns do not rely on excitation wavelength and always possess the same mode.

To find the relationship between polarization-dependent SHG/THG patterns and excitation wavelength, uniaxial tensile strain ~ 0.9% is applied onto monolayer WS_2 to break the three-fold rotation symmetry as well as mirror symmetry

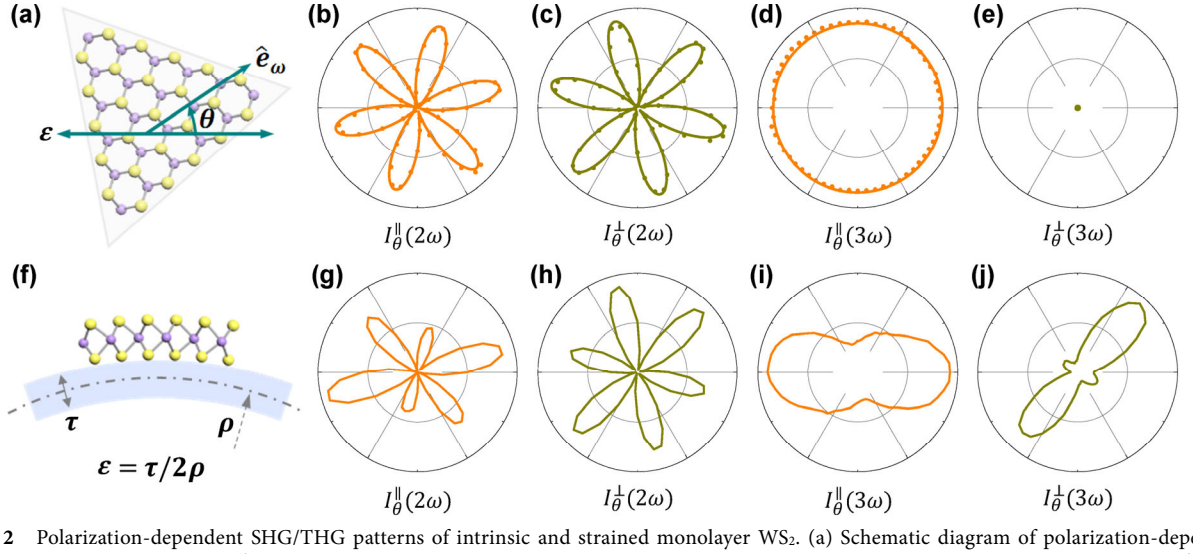

Figure 2 Polarization-dependent SHG/THG patterns of intrinsic and strained monolayer WS_2. (a) Schematic diagram of polarization-dependent SHG/THG from monolayer WS_2. $\hat{\boldsymbol{e}}_{\omega}$ is the polarization direction of linear excitation laser in lab coordinates. θ is the polarization angle of $\hat{\boldsymbol{e}}_{\omega}$ from the horizontal direction. Uniaxial tensile strain ε is always along horizontal direction. (b) and (c) Parallel component (b) $I_{\theta}^{\parallel}(2\omega)$ and perpendicular component (c) $I_{\theta}^{\perp}(2\omega)$ of polarization-dependent SHG pattern from intrinsic monolayer WS_2. The excitation pulse laser wavelength is ~ 1,290 nm and ω is corresponding light frequency. (d) and (e) Parallel component (d) $I_{\theta}^{\parallel}(3\omega)$ and perpendicular component (e) $I_{\theta}^{\perp}(3\omega)$ of the polarization-dependent THG pattern from intrinsic monolayer WS_2. (f) Schematic diagram of strain apparatus and uniaxial tensile strain ε ~ 0.9% could be applied to monolayer WS_2 by bending the flexible substrate. (g)–(j) Polarization-dependent SHG/THG patterns (g) $I_{\theta}^{\parallel}(2\omega)$, (h) $I_{\theta}^{\perp}(2\omega)$, (i) $I_{\theta}^{\parallel}(3\omega)$, and (j) $I_{\theta}^{\perp}(3\omega)$ from strained monolayer WS_2.

about *bc* plane (Fig. 2(f)). The crystallographic point group is reduced to C_{1h} so that all elements in $\chi^{(2)}_{strain}$ or $\chi^{(3)}_{strain}$ tensor becomes non-zero as shown in Eq. (2) and no constraint between them exists. Therefore, the polarization-dependent SHG/THG patterns of strained WS_2 follows Eq. (3): SHG patterns $I^{\parallel}_{\theta}(2\omega)$ and $I^{\perp}_{\theta}(2\omega)$ deform into six asymmetric petals (Figs. 2(g) and 2(h)); while THG patterns shows anisotropy: the long-axis of $I^{\parallel}_{\theta}(3\omega)$ indicates strain direction and $I^{\perp}_{\theta}(3\omega)$ stretches out four asymmetric petals [26].

3.3 SHG/THG pattern evolution of strained monolayer WS_2 under different excitonic resonance states

As we shall see in the following, although excitonic effects never change the crystallographic symmetry of strained monolayer WS_2 (C_{1h} point group), polarization-dependent SHG/THG patterns are remarkably modulated by excitation wavelength due to excitonic resonance. Uniaxial tensile strain also perturbs the band structure of monolayer WS_2 and leads to the reduction of optical bandgap (~ 662 nm, Fig. S1 in the Electronic Supplementary Material (ESM)). Figure 3 summarizes polarization-dependent SHG/THG patterns around two-photon excitonic resonance when the two-photon energy of excitation wavelength λ_{ex} = 1,310 nm/1,330 nm/1,350 nm is larger than/comparable to/smaller than the optical bandgap. The SHG patterns $I^{\parallel}_{\theta}(2\omega)$ (Figs. 3(b), 3(g), and 3(l)) and $I^{\perp}_{\theta}(2\omega)$ (Figs. 3(c), 3(h), and 3(m)) always have the same polarization dependence regardless of the excitation wavelength. On the contrary, it is striking that polarization-dependent THG patterns have a dramatical evolution. The $I^{\parallel}_{\theta}(3\omega)$ pattern has a dumbbell shape with long-axis along strain direction (Fig. 3(d), λ_{ex} = 1,310 nm). However, it deforms into a bow-tie shape around two-photon excitonic resonance (Fig. 3(i), λ_{ex} = 1,330 nm) and finally gets back to the dumbbell shape but the long-axis has a 90° flip (Fig. 3(n), λ_{ex} = 1,350 nm). The $I^{\perp}_{\theta}(3\omega)$ pattern also undergoes an obvious evolution: the long-axis and short-axis of the asymmetric four-petal pattern interchange with each other (Figs. 3(e), 3(j), and 3(o)). Furthermore, when the excitation wavelength continues to be longer even to three-photon excitonic resonance (λ_{ex} = 1,780 nm/1,924 nm/ 1,990 nm), both polarization-dependent SHG and THG modes no longer change (Fig. 4 and Fig. S2 in the ESM). Limited by the available excitation wavelength, strained $MoSe_2$ (optical bandgap ~ 800 nm) is chosen to investigate one-photon excitonic resonance, and SHG patterns keep the same polarization dependence (Fig. S3 in the ESM). In summary, only giant THG pattern evolution of strained monolayer WS_2 is observed at two-photon excitonic resonance.

From a qualitative point of view, since the second/third order nonlinear susceptibility of intrinsic monolayer WS_2 has only one independent variable *A* or *B*, polarization-dependent SHG/THG patterns are supposed to remain unchanged even if the magnitude of *A* or *B* varies due to different excitonic resonance. When uniaxial tensile strain reduces crystallographic symmetry of monolayer WS_2, the constraint between nonlinear susceptibility tensor elements is broken, and the variation of each tensor element magnitude could be different. As a result, it is normal to observe variation in SHG/THG polarization behaviors. On the one hand, excitonic resonance usually leads to dramatically enhancement of magnitude of nonlinear susceptibility in a narrow band [14–17]. Therefore, the relative change of susceptibility tensor elements is more likely to be magnified around excitonic resonance. As a result, the giant pattern evolution of nonlinear optical response only occurs at

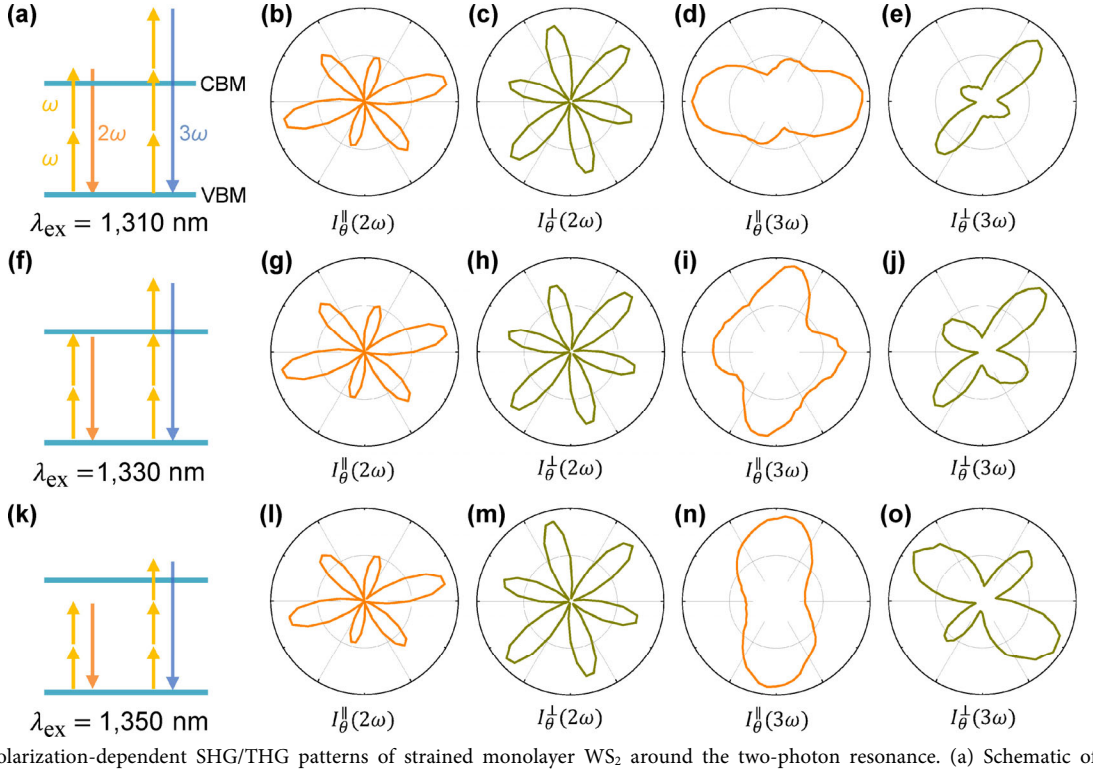

Figure 3 Polarization-dependent SHG/THG patterns of strained monolayer WS_2 around the two-photon resonance. (a) Schematic of SHG/THG process in strained monolayer WS_2 when two-photon energy of the excitation light (λ_{ex} = 1,310 nm) is larger than the optical bandgap of strained monolayer WS_2. Two horizontal lines represent conduction band minimum (CBM) and valence band maximum (VBM) of strained monolayer WS_2, respectively. The yellow, orange and blue arrows indicate the excitation light (ω) and generated SHG signal (2ω) and THG signal (3ω). (b)–(e) Polarization-dependent SHG/THG patterns (b) $I^{\parallel}_{\theta}(2\omega)$, (c) $I^{\perp}_{\theta}(2\omega)$, (d) $I^{\parallel}_{\theta}(3\omega)$, (e) $I^{\perp}_{\theta}(3\omega)$ of strained WS_2 as shown in (a). (f)–(o) Polarization-dependent SHG/THG patterns of strained WS_2 (f)–(j) near two-photon resonance (λ_{ex} = 1,330 nm) and (k)–(o) the two-photon energy of excitation light (λ_{ex} = 1,350 nm) is smaller than the optical bandgap.

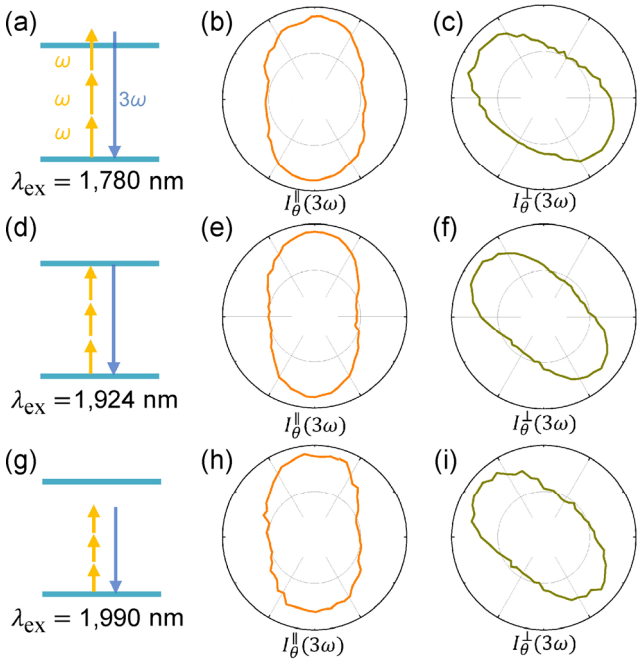

Figure 4 Polarization-dependent THG patterns of strained monolayer WS_2 around the three-photon resonance. (a) Schematic of SHG/THG process in strained monolayer WS_2 when three-photon energy of the excitation light ($\lambda_{ex} = 1{,}780$ nm) is larger than the optical bandgap of strained WS_2. (b) and (c) Polarization-dependent THG patterns (b) $I_{\theta}^{\parallel}(3\omega)$, (c) $I_{\theta}^{\perp}(3\omega)$ of strained WS_2 as shown in (a). (d)–(i) Polarization-dependent THG patterns of strained monolayer WS_2 (d)–(f) near three-photon resonance ($\lambda_{ex} = 1{,}924$ nm) and (g)–(i) the three-photon energy of the excitation light ($\lambda_{ex} = 1{,}990$ nm) is smaller than the optical bandgap.

excitonic resonance. On the other hand, the third-order nonlinear susceptibility is a four-rank tensor which has more independent variables than that in the three-rank second-order nonlinear susceptibility tensor. Hence compared with SHG, it is reasonable that THG is more sensitive or has more possibility than SHG to undergo the evolution of polarization dependence near excitonic resonance. Here, we note that the *ab-initio* theory for understanding the specific nonlinear pattern evolution around excitonic resonance is still lacking. Our experimental study might provide powerful reference and evoke the further development of theoretical study of excitonic effect on the nonlinearity of 2D materials to unveil the underlying microscopic mechanism.

4 Conclusions

In summary, we demonstrate that excitonic effects have a significant modulation on polarization dependence of nonlinear response of strained monolayer WS_2 by excitation wavelength covering both two-photon and three-photon excitonic resonance conditions. SHG patterns stay almost unchanged regardless of excitation wavelength, guaranteeing the robustness of polarization-dependent SHG as a symmetry characterization method. In comparison, THG patterns are strongly dependent on the excitation wavelength, and go through a giant evolution near two-photon excitonic resonance. For future crystallographic symmetry characterization, our results indicate that excitonic effects should be carefully accounted for to avoid incorrect determination of related properties when using polarization-dependent nonlinear optical method. From a prospective point of view, our results not only exploit a novel approach to modulate anisotropic nonlinear optical response of 2D materials through effectively tuning the resonance state, but also accelerate new designs and applications in the future nonlinear optoelectronic devices based on the wide range of 2D materials.

Acknowledgements

This work was supported by the Key R&D Program of Guangdong Province (Nos. 2019B010931001, 2020B010189001, 2018B010109009, and 2018B030327001), the National Natural Science Foundation of China (Nos. 51991340 and 51991342), the National Key R&D Program of China (Nos. 2016YFA0300903 and 2016YFA0300804), Beijing Natural Science Foundation (No. JQ19004), Beijing Excellent Talents Training Support (No. 2017000026833ZK11), Beijing Municipal Science & Technology Commission (No. Z191100007219005), Beijing Graphene Innovation Program (No. Z181100004818003), Bureau of Industry and Information Technology of Shenzhen (Graphene platform 201901161512), Guangdong Innovative and Entrepreneurial Research Team Program (No. 2016ZT06D348), and the Science, Technology and Innovation Commission of Shenzhen Municipality (No. KYTDPT20181011104202253).

Electronic Supplementary Material: Supplementary material (nonlinear optical response of WS_2 and SHG polarization dependence of $MoSe_2$ around one-photon excitonic resonance) is available in the online version of this article at https://doi.org/10.1007/s12274-020-2995-2.

References

[1] Wooten, E. L.; Kissa, K. M.; Yi-Yan, A.; Murphy, E. J.; Lafaw, D. A.; Hallemeier, P. F.; Maack, D.; Attanasio, D.V.; Fritz, D. J.; McBrien, G. J. et al. A review of lithium niobate modulators for fiber-optic communications systems. *IEEE J. Sel. Top. Quant. Electron.* **2000**, *6*, 69–82.

[2] Keller, U. Recent developments in compact ultrafast lasers. *Nature* **2003**, *424*, 831–838.

[3] Li, C. F. *Nonlinear Optics: Principles and Applications*; Springer: Singapore, 2017.

[4] Autere, A.; Jussila, H.; Dai, Y. Y.; Wang, Y. D.; Lipsanen, H.; Sun, Z. P. Nonlinear optics with 2D layered materials. *Adv. Mater.* **2018**, *30*, 1705963.

[5] You, J. W.; Bongu, S. R.; Bao, Q.; Panoiu, N. C. Nonlinear optical properties and applications of 2D materials: Theoretical and experimental aspects. *Nanophotonics* **2019**, *8*, 63–97.

[6] Wen, X. L.; Gong, Z. B.; Li, D. H. Nonlinear optics of two-dimensional transition metal dichalcogenides. *InfoMat* **2019**, *1*, 317–337.

[7] Wang, J.; Hernandez, Y.; Lotya, M.; Coleman, J. N.; Blau, W. J. Broadband nonlinear optical response of graphene dispersions. *Adv. Mater.* **2009**, *21*, 2430–2435.

[8] Breusing, M.; Ropers, C.; Elsaesser, T. Ultrafast carrier dynamics in graphite. *Phys. Rev. Lett.* **2009**, *102*, 086809.

[9] Malard, L. M.; Alencar, T. V.; Barboza, A. P. M.; Mak, K. F.; de Paula, A. M. Observation of intense second harmonic generation from MoS_2 atomic crystals. *Phys. Rev. B* **2013**, *87*, 201401.

[10] Kumar, N.; Kumar, J.; Gerstenkorn, C.; Wang, R.; Chiu, H. Y.; Smirl, A. L.; Zhao, H. Third harmonic generation in graphene and few-layer graphite films. *Phys. Rev. B* **2013**, *87*, 121406.

[11] Kumar, N.; Najmaei, S.; Cui, Q. N.; Ceballos, F.; Ajayan, P. M.; Lou, J.; Zhao, H. Second harmonic microscopy of monolayer MoS_2. *Phys. Rev. B* **2013**, *87*, 161403.

[12] Wang, K. P.; Wang, J.; Fan, J. T.; Lotya, M.; O'Neill, A.; Fox, D.; Feng, Y. Y.; Zhang, X. Y.; Jiang, B. X.; Zhao, Q. Z. et al. Ultrafast saturable absorption of two-dimensional MoS_2 nanosheets. *ACS Nano* **2013**, *7*, 9260–9267.

[13] Wang, Q. H.; Kalantar-Zadeh, K.; Kis, A.; Coleman, J. N.; Strano, M. S. Electronics and optoelectronics of two-dimensional transition metal dichalcogenides. *Nat. Nanotechnol.* **2012**, *7*, 699–712.

[14] Trolle, M. L.; Seifert, G.; Pedersen, T. G. Theory of excitonic second-harmonic generation in monolayer MoS_2. *Phys. Rev. B* **2014**, *89*, 235410.
[15] Yin, X. B.; Ye, Z. L.; Chenet, D. A.; Ye, Y.; O'Brien, K.; Hone, J. C.; Zhang, X. Edge nonlinear optics on a MoS_2 atomic monolayer. *Science* **2014**, *344*, 488–490.
[16] Wang, G.; Marie, X.; Gerber, I.; Amand, T.; Lagarde, D.; Bouet, L.; Vidal, M.; Balocchi, A.; Urbaszek, B. Giant enhancement of the optical second-harmonic emission of WSe_2 monolayers by laser excitation at exciton resonances. *Phys. Rev. Lett.* **2015**, *114*, 097403.
[17] Seyler, K. L.; Schaibley, J. R.; Gong, P.; Rivera, P.; Jones, A. M.; Wu, S. F.; Yan, J. Q.; Mandrus, D. G; Yao, W.; Xu, X. D. Electrical control of second-harmonic generation in a WSe_2 monolayer transistor. *Nat. Nanotechnol.* **2015**, *10*, 407–411.
[18] Rodrigues, S. P.; Cai, W. S. Nonlinera optics: Tuning harmonics with excitons. *Nat. Nanotechnol.* **2015**, *10*, 387–388.
[19] Xiao, J.; Zhao, M.; Wang, Y.; Zhang, X. Excitons in atomically thin 2D semiconductors and their applications. *Nanophotonics* **2017**, *6*, 1309–1328.
[20] Mueller, T.; Malic, E. Exciton physics and device application of two-dimensional transition metal dichalcogenide semiconductors. *NPJ 2D Mater. Appl.* **2018**, *2*, 29.
[21] Shen, Y. R. *The Principles of Nonlinear Optics*; Wiley: New York, 1984.
[22] Boyd, R. W. *Nonlinear Optics*; Academic, 2014.
[23] Tran, V.; Soklaski, R.; Liang, Y. F.; Yang, L. Layer-controlled band gap and anisotropic excitons in few-layer black phosphorus. *Phys. Rev. B* **2014**, *89*, 235319.
[24] Hsu, W. T.; Zhao, Z. A.; Li, L. J.; Chen, C. H.; Chiu, M. H.; Chang, P. S.; Chou, Y. C.; Chang, W. H. Second harmonic generation from artificially stacked transition metal dichalcogenide twisted bilayers. *ACS Nano* **2014**, *8*, 2951–2958.
[25] Liang, J.; Zhang, J.; Li, Z. Z.; Hong, H.; Wang, J. H.; Zhang, Z. H.; Zhou, X.; Qiao, R. X.; Xu, J. Y.; Gao, P. et al. Monitoring local strain vector in atomic-layered $MoSe_2$ by second-harmonic generation. *Nano Lett.* **2017**, *17*, 7539–7543.
[26] Liang, J.; Wang, J. H.; Zhang, Z. H.; Su, Y. Z.; Guo, Y.; Qiao, R. X.; Song, P. Z.; Gao, P.; Zhao, Y.; Jiao, Q. Z. et al. Universal imaging of full strain tensor in 2D crystals with third-harmonic generation. *Adv. Mater.* **2019**, *31*, 1808160.
[27] Sie, E. J.; Nyby, C. M.; Pemmaraju, C. D.; Park, S. J.; Shen, X. Z.; Yang, J.; Hoffmann, M. C.; Ofori-Okai, B. K.; Li, R. K.; Reid, A. H. et al. An ultrafast symmetry switch in a Weyl semimetal. *Nature* **2019**, *565*, 61–66.
[28] Ramasubramaniam, A. Large excitonic effects in monolayers of molybdenum and tungsten dichalcogenides. *Phys. Rev. B* **2012**, *86*, 115409.
[29] Ye, Z. L.; Cao, T.; O'Brien, K.; Zhu, H. Y.; Yin, X. B.; Wang, Y.; Louie, S. G.; Zhang, X. Probing excitonic dark states in single-layer tungsten disulphide. *Nature* **2014**, *513*, 214–218.
[30] Janisch, C.; Wang, Y. X.; Ma, D.; Mehta, N.; Elías, A. L.; Perea-López, N.; Terrones, M.; Crespi, V.; Liu, Z. W. Extraordinary second harmonic generation in tungsten disulfide monolayers. *Sci. Rep.* **2015**, *4*, 5530.
[31] Torres-Torres, C.; Perea-López, N.; Elías, A. L.; Gutiérrez, H. R.; Cullen, D. A.; Berkdemir, A.; López-Urías, F.; Terrones, H.; Terrones, M. Third order nonlinear optical response exhibited by mono- and few-layers of WS_2. *2D Mater.* **2016**, *3*, 021005.